

Discrepancies between transcutaneous and estimated glomerular filtration rates in rats with chronic kidney disease



see commentary on page 1159

OPEN

Tobias T. Pieters^{1,4}, Paul J. Besseling^{1,4}, Dominique M. Bovée², Maarten B. Rookmaaker¹, Marianne C. Verhaar¹, Benito Yard³, Ewout J. Hoorn² and Jaap A. Joles¹

¹Department of Nephrology and Hypertension, University Medical Center Utrecht, Utrecht, The Netherlands; ²Division of Nephrology and Transplantation, Department of Internal Medicine, Erasmus Medical Center, University Medical Center Rotterdam, Rotterdam, The Netherlands; and ³Department of Medicine, University Hospital Mannheim, University of Heidelberg, Mannheim, Germany

Accurate assessment of the glomerular filtration rate (GFR) is crucial for researching kidney disease in rats. Although validation of methods that assess GFR is crucial, large-scale comparisons between different methods are lacking. Both transcutaneous GFR (tGFR) and a newly developed estimated GFR (eGFR) equation by our group provide a low-invasive approach enabling repeated measurements. The tGFR is a single bolus method using FITC-labeled sinistrin to measure GFR based on half-life of the transcutaneous signal, whilst the eGFR is based on urinary sinistrin clearance. Here, we retrospectively compared tGFR, using both 1- and 3- compartment models (tGFR_{1c} and tGFR_{3c}, respectively) to the eGFR in a historic cohort of 43 healthy male rats and 84 male rats with various models of chronic kidney disease. The eGFR was on average considerably lower than tGFR-1c and tGFR-3c (mean differences 855 and 216 $\mu\text{L}/\text{min}$, respectively) and only 20 and 47% of measurements were within 30% of each other, respectively. The relative difference between eGFR and tGFR was highest in rats with the lowest GFR. Possible explanations for the divergence are problems inherent to tGFR, such as technical issues with signal measurement, description of the signal kinetics, and translation of half-life to tGFR, which depends on distribution volume. The unknown impact of isoflurane anesthesia used in determining mGFR remains a limiting factor. Thus, our study shows that there is a severe disagreement between GFR measured by tGFR and eGFR, stressing the need for more rigorous validation of the tGFR and possible adjustments to the underlying technique.

Kidney International (2024) **105**, 1212–1220; <https://doi.org/10.1016/j.kint.2024.02.020>

KEYWORDS: estimated glomerular filtration rate; FITC-sinistrin; sinistrin clearance; rats; transcutaneous glomerular filtration rate

Correspondence: Jaap A. Joles, University Medical Center Utrecht, Department of Nephrology and Hypertension (F03.223), POB 85500, 3508 GA Utrecht, The Netherlands. E-mail: J.A.Joles@umcutrecht.nl

⁴Contributed equally.

Received 5 June 2023; revised 3 February 2024; accepted 12 February 2024; published online 19 March 2024

Copyright © 2024, International Society of Nephrology. Published by Elsevier Inc. This is an open access article under the CC BY license (<http://creativecommons.org/licenses/by/4.0/>).

Translational Statement

Glomerular filtration rate (GFR) is the most important measure of kidney function. Its application in animal models for studying kidney disease is crucial. In this study, we evaluated the accuracy of transcutaneous GFR (tGFR) compared to urine sinistrin-validated estimated GFR in male rats. We observed a marked discrepancy between these 2 methods. Problems inherent to the tGFR probably underlie this discrepancy. Results of this study may lead to increased accuracy of GFR assessment in rats, facilitating animal models that provide insights into the pathophysiology of kidney disease and the development of new treatments that may translate to the clinic.

The rat is used frequently as an experimental model in a wide range of kidney diseases. Accurate assessment of kidney function in single or repeated measurements is a vital part of these studies,¹ and it is best quantified by the glomerular filtration rate (GFR). GFR cannot be measured directly, but it can be assessed from the measured clearance of exogenous filtration markers (that is, measured GFR [mGFR]) or can be estimated from serum levels of endogenous filtration markers (that is, estimated GFR [eGFR]).² The GFR is used mainly to identify the severity of kidney disease and the effectiveness of an intervention. The gold standard for measuring GFR is the urinary sinistrin clearance (mGFR), a laborious and specialized measurement. Many alternatives are available that measure GFR using other exogenous filtration markers, such as iohexol,³ urinary clearance of fluorescein isothiocyanate-labeled sinistrin (FITC-S),⁴ or transcutaneous measurements of fluorescently labeled filtration markers (tGFR).^{2,5} In 2021, we developed and validated an equation that estimates GFR in male rats, using the readily available variables plasma creatinine, plasma urea, and body weight, with urinary sinistrin clearance as a reference standard.⁶ Subsequently, this equation

was applied by other groups.^{7–13} A new method, such as tGFR, which is currently used widely in rat experiments, entails a need for standardization to enable comparison of the results from different labs, and with other methods of assessing GFR. Currently, the tGFR has not been compared extensively to another method of assessing GFR, nor has it been compared among different investigators at different labs. Thorough validation in a wide range of disease models and rat strains is certainly needed.

The tGFR method using FITC-S is used widely as a noninvasive alternative to mGFR in rodents.⁵ Commercially available kits using FITC-S allow for transcutaneous measurement of the half-life, which can be converted to tGFR using a measure of volume of distribution without blood sampling.¹⁴ However, certain technical challenges are associated with the use of transcutaneous methods and bolus injection measurements.^{15,16} These challenges include the following: the transcutaneous signal has to be accurately measured; the attenuation of the signal should be attributed entirely to GFR elimination; and the volume of distribution has to be estimated accurately to convert signal half-life to GFR. The tGFR method uses a single-bolus intravenous infusion of FITC-S, after which the transcutaneous signal is described as a fast distribution phase in which FITC-S spreads in the volume of distribution, followed approximately 45 minutes later by a log-linear elimination phase, which is used to calculate half-life.⁵ To describe the kinetics of FITC-S, models using up to 3 compartments have been suggested, although the 1-compartment model is the one used most widely.¹⁷ The volume of distribution is assumed to be equal for all rats and was estimated in the original paper to be 31.26 ml/100 g bodyweight. The tGFR is calculated by dividing this volume of distribution by the signal half-life. Although the measure of volume of distribution was assessed in the original paper, it may differ among rat strains and disease models, which may bias the tGFR significantly. Furthermore, technical concerns have been raised previously regarding the use of transcutaneous measurement of FITC-S.^{17,18} Although the tGFR provided unbiased results in the original study in which it was developed, whether it is unbiased, compared to other methods of measuring GFR, or when measured by different research groups is not clear.^{14,15}

The goal of this study was to compare tGFR to eGFR in rats, providing a comparison among different methods to assess GFR in a large group of animals. To this end, we evaluated the association between endogenous filtration markers (creatinine and urea) and mGFR in the dataset with which the eGFR was developed ($n = 441$), and compared this to the association between the endogenous filtration markers and the tGFR, using both 1- and 3-compartment models (tGFR_1c and tGFR_3c), in a separate historic dataset from 2 experiments in rats with a variable degree of renal insufficiency ($n = 127$).^{19,20} Furthermore, we compared the eGFR and both tGFR_1c and tGFR_3c in simultaneous measurements using the same historic dataset ($n = 127$).

METHODS

Experimental animals

All rats in the selected studies^{21–28} and all unpublished data (Supplementary Table S1) were used in agreement with the law on animal experiments in The Netherlands. We compared the tGFR to the eGFR in a cohort that aggregated the data of 2 studies performed in the Erasmus Medical Center (Rotterdam, The Netherlands); tGFR, creatinine, and urea were measured (the tGFR cohort, $n = 127$). The eGFR was developed in a cohort (the mGFR cohort, $n = 441$) that aggregated data from 10 studies with various disease models, all performed in the University Medical Center Utrecht, Utrecht, The Netherlands.⁶ Both the tGFR and the mGFR cohort contained diseased as well as healthy control animals (disease models are specified in Supplementary Table S1). All measurements of tGFR, mGFR, creatinine, and urea were done using the same protocols in all animals.

Measurement of urinary sinistrin clearance and endogenous filtration markers

Urinary sinistrin clearance was used to obtain mGFR. For the urinary sinistrin clearance, rats were anesthetized with isoflurane (4% induction, and 2.5% maintenance) mixed with 100% O₂ (0.3 l/min) with an Isoflurane Vaporizer (UNO Life Science Solutions) and artificially ventilated. This set-up previously provided adequate oxygenation.²⁹ To compensate for fluid loss during the experiment, animals received an intravenous infusion of 150 mmol/l NaCl (containing 6% bovine serum albumin before surgery, and 1% after surgery) at a rate of 10 $\mu\text{l} \cdot \text{min}^{-1} \cdot 100 \text{ g bw}^{-1}$. The femoral artery was cannulated for collection of blood plasma and arterial pressure measurement. The mean arterial pressure was within range of GFR autoregulation (mean arterial pressure, 80–160 mm Hg). Immediately after placement of the femoral arterial cannula, the first blood sample (300 μl) was drawn for the determination of baseline levels of plasma sinistrin, creatinine, and urea. The jugular vein was cannulated for continuous infusion of sinistrin (Inutest, Fresenius Kabi). Urine was collected from the bladder. After 60 minutes of stabilization, a second blood sample (300 μl) was taken, immediately followed by collection of urine for 2 periods of 15 minutes each. After the second period, a third blood sample (300 μl) was taken. Urine and plasma samples were analyzed for sinistrin (by measuring fructose photometrically with Indole 3-acetic acid after hydrolyzation of sinistrin).³⁰ The renal clearance data shown are averaged data of the 2 consecutive 15-minute urine collections. Plasma creatinine was measured with an enzymatic colorimetric assay with the DiaSys Creatinine PAP FS kit (DiaSys Diagnostic Systems GmbH). Plasma urea was determined with an enzymatic method with DiaSys Urea CT FS (DiaSys Diagnostic Systems GmbH). The eGFR was calculated using the following equations⁶: plasma creatinine $< 52 \mu\text{mol/l}$: $\text{eGFR} = 880 \times W^{0.695} \times C^{-0.660} \times U^{-0.391}$; and plasma creatinine $\geq 52 \mu\text{mol/l}$: $\text{eGFR} = 5862 \times W^{0.695} \times C^{-1.150} \times U^{-0.391}$, where eGFR = estimated glomerular filtration rate ($\mu\text{l}/\text{min}$), W = weight (grams), C = creatinine ($\mu\text{mol}/\text{l}$), and U = urea (mmol/l).

Measurement of transcutaneous filtration markers

For the tGFR measurements, rats were anesthetized lightly with isoflurane and were artificially ventilated using a nose cone for approximately 10 minutes. During anesthesia, the cutaneous fluorescent detection device (Mannheim Pharma & Diagnostics GmbH) was attached to a depilated region on the back of the rat using a double-sided adhesive patch. The FITC-S bolus (0.24 mg/kg dissolved in saline) was injected via the tail vein during this light

Table 1 | Cohort characteristics

Variable	mGFR, $\mu\text{l}/\text{min}$ (UMCU)		tGFR, ml/min (Erasmus)	
Rat numbers	441		127	
mGFR, ml/min	1441	(909, 2132)	—	—
tGFR, 1-compartment, $\mu\text{l}/\text{min}$	—	—	1915	(1439, 3666)
tGFR, 3-compartment, $\mu\text{l}/\text{min}$	—	—	1569	(996, 2700)
eGFR, $\mu\text{l}/\text{min}$	1580	(1120, 1994)	1141	(596, 2960)
Body weight, g	361	(321, 394)	400	(369, 428)
Plasma creatinine, $\mu\text{mol}/\text{l}$	53	(38, 69)	64	(31, 93)
Plasma urea, mmol/l	11	(9, 15)	13	(7, 20)
Rat strain (FHH, Lewis, Sprague-Dawley, Wistar)	24, 301, 80, 26		0, 0, 127, 0	

eGFR, estimated GFR; Erasmus, Erasmus Medical Center, University Medical Center Rotterdam, Rotterdam, The Netherlands; FHH, fawn-hooded hypertensive; GFR, glomerular filtration rate; mGFR, measured glomerular filtration rate; tGFR, transcutaneous glomerular filtration rate; UMCU, University Medical Center Utrecht, Utrecht, The Netherlands. Data are shown as medians (interquartile ranges), unless otherwise indicated.

anesthesia, to enhance both the rat’s comfort and the precision of the injection procedure, thus avoiding s.c. infusion. After administration of the FITC-S bolus, rats were allowed to wake and roam freely for 2 hours, after which the device was removed. Using partner software for the fluorescent detection device (Mannheim Pharma & Diagnostics GmbH), an elimination kinetics curve for FITC-S was generated. tGFR was calculated using the excretion half-life ($t_{1/2}$) of FITC-S, calculated with the 1-compartment model and the 3-compartment model without linear correction (as several elimination curves did not reach baseline, which is a requirement for linear correction) and converted to tGFR with their respective conversion factors. For the 1-compartment model, we used the following: tGFR_{1c} (ml/min per 100 g body weight) = 31.26 ($\text{ml}/100$ g body weight)/ $t_{1/2}$ FITC-S (minutes). For the 3-compartment model, we used the following: tGFR_{3c} (ml/min per 100 g body weight) = 21.33 ($\text{ml}/100$ g body weight)/ $t_{1/2}$ FITC-S (minutes).^{5,17} Then, 3 to 10 days (median, 6 days) after the tGFR measurements, rats were again anesthetized with isoflurane, followed immediately by collection of blood from the inferior vena cava for measurement of creatinine and urea. One researcher (TTP) evaluated the intensity curves on a log scale to evaluate curve shapes.

Comparison between tGFR and eGFR

The development and validation of the eGFR equation have been described previously.⁶ Bias was assessed by calculating mean prediction error ($\text{tGFR} - \text{eGFR}$); precision was assessed by calculating the R^2 value using ordinary linear regression; and accuracy was assessed by the mean absolute percentage error (MAPE), the root mean squared error (RMSE), and the number of predictions that fell within 15% and 30% of the estimate (P15, P30). Point estimates and 95% confidence intervals (CIs) were calculated with bootstrap (1000 \times). We computed CIs using bootstrap (1000 \times). For P15 and P30, we used the normal approximation. The association between creatinine/urea and mGFR/tGFR was visualized with scatter plots using log/log scales and locally estimated scatterplot smoothing (LOESS) regression lines. Accuracy was visualized using difference plots with a smoothed regression line, and 95% CI was calculated using quantile regression. The ability of the eGFR and tGFR to discriminate healthy from diseased animals was tested with the 2-sided independent t test comparing Cohen’s d and visualized with combined density and rug plots. In rats in which urinary sinistrin clearance was measured, the stability of plasma creatinine during anesthesia was assessed with scatter plots, and the 2-sided paired t test. Differences in frequency between groups were evaluated with

Fisher’s exact test for count data. Mean differences between groups were tested with a 2-way analysis of variance with *post hoc* analyses with the Tukey test. P values below 0.05 were considered significant. All computations and statistics were performed using R, version 4.1.3 (R Foundation for Statistical Computing).

RESULTS

Rat cohorts

We analyzed the data of 568 rats divided over 2 different cohorts consisting of healthy and diseased rats; the mGFR cohort ($n = 441$) and the tGFR cohort ($n = 127$; Table 1). In the mGFR cohort, the mGFR ranged from 33 $\mu\text{l}/\text{min}$ to 4378 $\mu\text{l}/\text{min}$ (median: 1441 $\mu\text{l}/\text{min}$, interquartile range: 909–2132 $\mu\text{l}/\text{min}$); in the tGFR cohort, tGFR_{1c} ranged from 517 $\mu\text{l}/\text{min}$ to 7497 $\mu\text{l}/\text{min}$ (median: 1915 $\mu\text{l}/\text{min}$, interquartile range: 1439–3666 $\mu\text{l}/\text{min}$), and tGFR_{3c} ranged from 328 $\mu\text{l}/\text{min}$ to 5571 $\mu\text{l}/\text{min}$ (median 1569, interquartile range: 996–2700 $\mu\text{l}/\text{min}$).

Comparison of sinistrin clearance and tGFR versus endogenous filtration markers and eGFR

Sinistrin clearance and tGFR were compared against the endogenous filtration markers creatinine and urea (Figure 1a). In relation to both markers, the tGFR consistently showed higher values, compared to the mGFR, with increasing discrepancy in rats with the highest creatinine and urea levels, as illustrated by the local regression lines (Figure 1a). This increasing divergence is also shown in a side-to-side comparison of the tGFR to the eGFR in the tGFR cohort, as illustrated by linear regression on the log-transformed values (Figure 1b; slope of regression line calculated with ordinary least-squared regression 0.59 for the tGFR_{1c} and 0.60 for the tGFR_{3c}), and a difference plot on a normal scale (Figure 1b). On average, the eGFR was lower than the tGFR_{1c} (mean difference, 855 $\mu\text{l}/\text{min}$) and the tGFR_{3c} (mean difference, 216 $\mu\text{l}/\text{min}$). Comparable precision was achieved with the tGFR_{1c} ($R^2 = 0.68$) and the tGFR_{3c} ($R^2 = 0.70$). Furthermore, only 20% of the eGFR values were within 30% of the tGFR_{1c} values (P30 = 20%), and 47% were within 30% of the tGFR_{3c} values (P30 = 47%; Table 2).

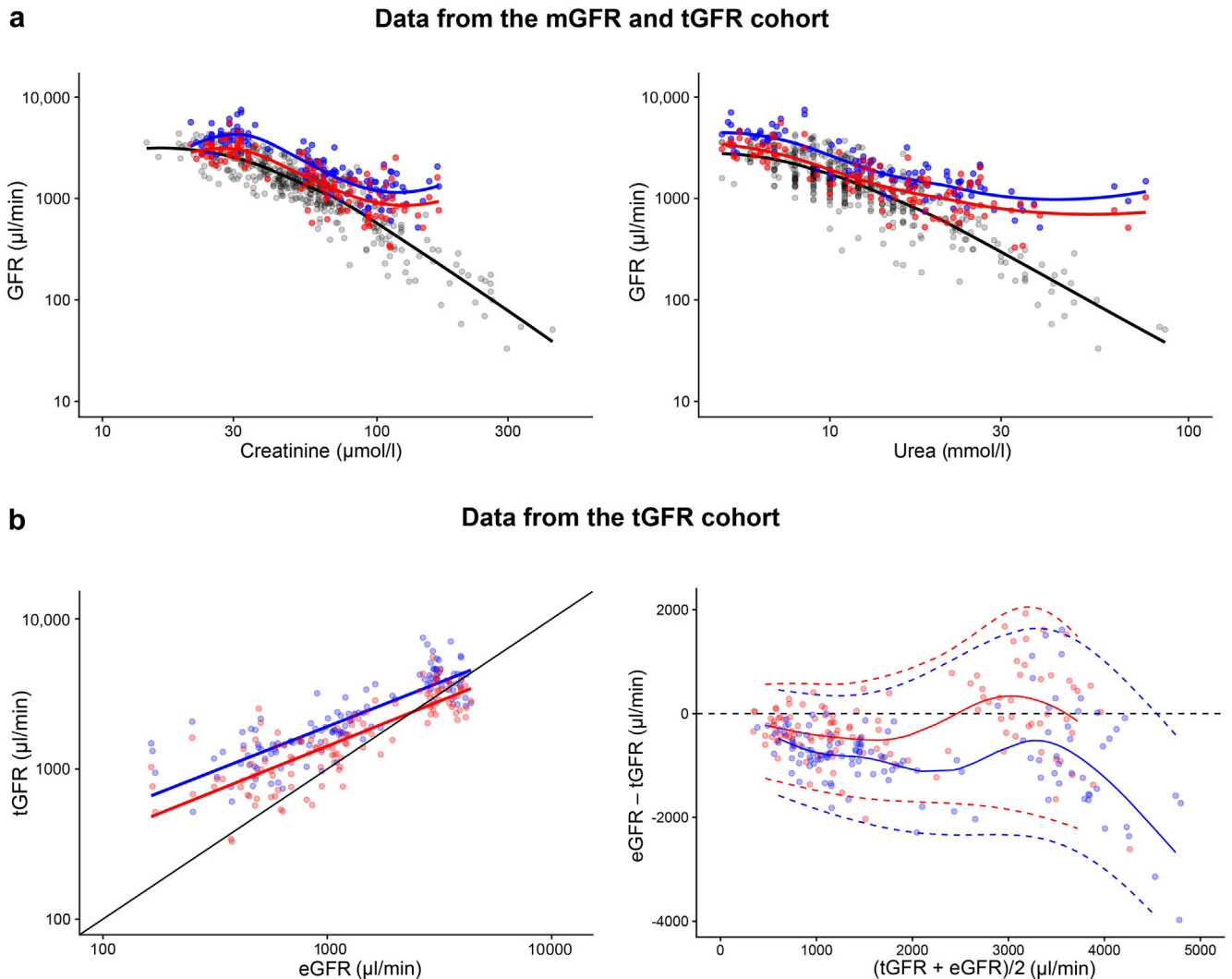


Figure 1 | (a) Scatter plots comparing endogenous filtration markers (creatinine, urea) with measured (m) glomerular filtration rate (GFR), measured by urinary sinistrin clearance and by transcutaneous fluorescein isothiocyanate-labeled sinistrin (FITC-S; (tGFR) using the 1-compartment model (tGFR_1c) or the 3-compartment model (tGFR_3c). Data and regression lines from the mGFR cohort are depicted in black; those from the tGFR cohort are shown in blue (tGFR_1c) and red (tGFR_3c). The y-axes show mGFR and tGFR; the x-axes show plasma creatinine ($\mu\text{mol/l}$; left panel) and plasma urea (mmol/l ; right panel). The lines are smoothed regression lines calculated with locally estimated scatterplot smoothing (LOESS). (b) Comparison between tGFR_1c (blue), tGFR_3c (red), and the estimated GFR (eGFR; black). The left panel shows a direct log-log comparison between eGFR ($\mu\text{l/min}$; x-axis) and tGFR ($\mu\text{l/min}$; y-axis), the line of identity (black solid line), and a regression lined calculated with ordinary least-squared regression (red or blue solid line). The right panel shows a difference plot of tGFR – eGFR, with the difference given on the y-axis, and the mean of eGFR and tGFR given on the x-axis. The lines were calculated using quantile regression (dashed lines represent the 2.5% and 97.5% quantile, respectively; the solid line represents the 50% quantile; blue indicates data for the tGFR 1-compartment method; red indicates data for the tGFR 3-compartment method).

A difference between tGFR and eGFR may be affected by measurement errors of the mGFR upon which the eGFR is based. Theoretically, the use of anesthesia during the assessment of mGFR may depress GFR and thereby introduce a biased estimate. To evaluate whether anesthesia may have affected the GFR during mGFR measurement, we compared the plasma creatinine level at the beginning (approximately 10 to 20 minutes after induction of anesthesia) to the plasma creatinine level at the end of the experiment (approximately 1.5–2 hours after induction of anesthesia). On average, we observed no significant change in creatinine level between

these 2 time points (mean increase, $0.61 \mu\text{mol/l}$, paired t test $P = 0.16$; [Supplementary Figure S1](#)).

Next, we evaluated the ability of tGFR and eGFR to discriminate between the diseased ($n = 84$) and the control animals ($n = 43$) in simultaneous measurements ($n = 127$; tGFR cohort). Although both had excellent discriminative ability to identify diseased from healthy animals, the eGFR displayed complete separation, whereas both the tGFR_1c and tGFR_3c had overlapping distribution curves ([Figure 2](#)). Furthermore, the eGFR had a larger difference in means between the diseased and control groups ($831 \mu\text{l/min}$ vs. 3341

Table 2 | Comparison of the tGFR, 1-compartment method (tGFR_1c), and the tGFR, 3-compartment method (tGFR_3c), against eGFR as a reference method

Method	Bias	Precision	Accuracy			
	MPE, µl/min	R2	RMSE, µl/min	MAPE	P15	P30
tGFR_1c	855 (698–1007)	0.68 (0.53–0.76)	1221 (1020–1440)	100 (79–123)	13 (6–19)	20 (13–27)
tGFR_3c	216 (91–332)	0.70 (0.59–0.76)	735 (625–852)	50 (34–68)	24 (17–31)	47 (39–56)

CI, confidence interval; eGFR, estimated glomerular filtration rate; MAPE, mean absolute percentage error; MPE, mean prediction error; P15, P30, percentage of points that fall within 15% and 30%, respectively, of the outcome; R2, R2 value calculated with linear regression; RMSE, root mean squared error; tGFR, transcutaneous glomerular filtration rate.

95% CIs are given in parentheses; these were calculated with bootstrap (1000×) using the normal confidence interval.

µl/min; Cohen’s d, −5.64 [95% CI: −6.43; −4.86]) than with the tGFR_1c (1635 µl/min vs. 4293 µl/min; Cohen’s d, −3.18 [95% CI: −3.71; −2.64]) and tGFR_3c (1251 vs. 3171 µl/min; Cohen’s d, −3.1 [95% CI: −3.63; −2.57]; **Figure 2**). In control rats, some tGFR measurements were >5000 µl/min. Such high values were not observed with eGFR (or mGFR).

Dosing curves

To investigate the discrepancy between tGFR and eGFR, we analyzed the raw data of transcutaneous FITC-sinistrin intensity. The plasma sinistrin concentration has been described previously as a fast distribution phase followed by a log-linear elimination phase (i.e., biphasic distribution),⁵ whereas in our rat cohort, we observed 4 shapes of fluorescence intensity (**Figure 3a**): monophasic elimination (*n* = 54); biphasic elimination (*n* = 39); late-monophasic elimination (*n* = 20; log-linear elimination occurs after more than 60 minutes after injection of the tracer); and an undefined shape (*n* = 14). First, we evaluated whether the curve shapes were associated with disease status. The biphasic curve shape had the most control animals compared to the other shapes (Fisher exact test *P* < 0.001). Next, we evaluated in which group the discrepancy between tGFR and eGFR was the highest. A significant difference was found between the relative difference between eGFR and tGFR_1c (log tGFR_1c/eGFR) and eGFR and tGFR_3c (log tGFR_3c/eGFR) when comparing the different shapes and when comparing controls and diseased animals (**Figure 3b**; 2-way analysis of variance for factor curve shape *P* < 0.001; for factor control/diseased *P* < 0.001 for both tGFR_1c and tGFR_3c). In the *post hoc* analysis, the smallest discrepancy was found in the biphasic group for both tGFR_1c (*post hoc* analysis biphasic vs undefined, *P* = 0.01; biphasic vs. late monophasic, *P* = 0.002; monophasic vs. biphasic, *P* = 0.03; all other combinations, *P* > 0.05) and tGFR_3c (*post hoc* analysis biphasic vs. undefined, *P* = 0.03; biphasic vs. late monophasic, *P* < 0.001; monophasic vs. late monophasic, *P* = 0.02; all other combinations, *P* > 0.05).

DISCUSSION

Accurate assessment of kidney function is essential in animal models used to study kidney disease. Although several methods are available to assess GFR, large-scale comparison among different methods to assess kidney function is lacking. In this study, we compared tGFR calculated with the 1-compartment model (tGFR_1c) and the 3-compartment

model (tGFR_3c) with a new eGFR equation. Our findings reveal a large discrepancy between eGFR and tGFR measurements, with both tGFR models consistently providing estimates higher than eGFR. Furthermore, this divergence increased with declining GFR. The fact that the eGFR equation was developed and validated against the gold-standard urinary sinistrin clearance in a large cohort of male rats with varying degrees of kidney disease raises concern that the tGFR may overestimate GFR systematically, especially in diseased animals.

Previous studies have focused on validation and resolution of technical challenges associated with tGFR. In the original paper, the tGFR_1c was developed in 20 healthy rats and validated by simultaneous enzymatic and fluorometric measurement of FITC-S in 7 healthy rats and 38 diseased rats. Although the tGFR provided unbiased results, compared to enzymatic sinistrin clearance, the enzymatic sinistrin clearance was calculated using the same fixed estimate of the volume of distribution and is therefore a validation of the half-life of sinistrin rather than GFR.⁵ Furthermore, no measure of accuracy, such as the P30, was calculated. A 3-compartment model (tGFR_3c) also was published, which did not vastly improve estimation of half-life on its own, but allowed for both a modulated baseline correction that improved accuracy and an improved estimate of the volume of distribution.¹⁷ This correction is needed, as the baseline fluorescence signal shifts after injection, compared to the initial baseline value before injection, which is attributed to photo-bleaching of the rat skin or the effects of the attachment of the device to the rat.¹⁷ The tGFR_3c was shown to be unbiased in 11 healthy animals against transcutaneous FITC-s clearance measured by continuous infusion, although no measure for accuracy, such as the P30, was calculated. In another study, the 1-compartment model was evaluated in simultaneous measurements, compared to an magnetic resonance imaging–based estimate of GFR, and tGFR_1c was found to be significantly higher than the magnetic resonance imaging values.³¹ We add to these observations that in a large retrospective cohort of healthy and diseased rats, a high level of bias and imprecision occurs for tGFR versus eGFR, which increases with worsening GFR. The tGFR_3c had better agreement with the eGFR, compared to the tGFR_1c, due to a substantial decrease in bias, whereas precision remained the same. Furthermore, qualitative assessment of the intensity curves revealed varying shapes, often without a clear log-linear elimination phase, making an

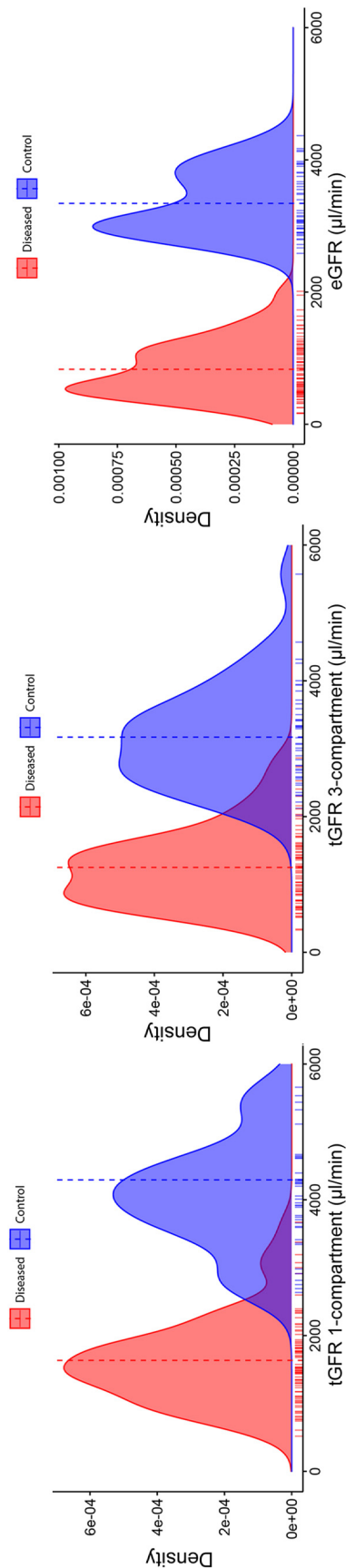


Figure 2 | Combined rug and density plots showing the difference in distribution between diseased (red) and control (blue) animals with transcutaneous glomerular filtration rate (tGFR), 1-compartment (left panel), tGFR, 3-compartment (middle panel), and estimated glomerular filtration rate (eGFR; right panel). The dashed line represents the mean.

assessment of an accurate half-life problematic. The measurements with the least bias, compared to the eGFR, were those for rats with a biphasic intensity curve, the shape that is described in the original paper, but this was found in a minority of rats in our cohort.

Several explanations for the discrepancy between the tGFR and the eGFR are possibilities. These explanations include measurement errors in mGFR, on which the eGFR is based, situations that may bias the eGFR, and measurement errors in the tGFR. The mGFR is measured in fully anesthetized animals, which may have affected the GFR (see the following paragraph), and therefore the eGFR. Although the eGFR was developed and shown to be accurate in a large cohort with different strains and disease models, it may have been affected by varying muscle mass of the animals, as is the case with creatinine-based equations in humans. We did not, however, include disease models that are associated with severe sarcopenia. Technical aspects of the transcutaneous measurements may have impacted our results. Fluorophores with an emission wavelength shorter than 600 nm, such as FITC, can encounter background autofluorescence of surrounding tissue, which impacts the accuracy of the measurement.¹⁸ Background autofluorescence can be decreased by providing a minimum distance between light emitting diode (LED) and photodiode (PD),³² although this is challenging in small animals. In addition, FITC is not an ideal fluorophore, as the penetration depth is limited.³³ This combination of high background, the required distance between the LED and PD, in combination with the limited penetration depth of FITC, may result in inaccurate measurements. Another difficulty in interpreting the tGFR is the fact that the volume of distribution of sinistrin, which is known to be equal to total extracellular water, is set for all rats of varying shapes, sizes, and strains when calculating the tGFR.^{5,34} Different rat strains, age, weight, and disease models, however, have a wide range of actual volumes of distribution, which can greatly affect GFR measurement. This impact is illustrated further by the large difference between the tGFR_{1c} and the tGFR_{3c}, which is explained mostly by a different estimate of the volume of distribution. In addition, the tGFR was developed in healthy rats only and assumes that the ratio between half-life and GFR is the same in healthy and diseased rats. This assumption may introduce bias when this is not the case—for example, if the speed of exchange differs among the different compartments, or the volume of distribution differs between healthy and diseased rats. In humans, the volume of distribution has been observed to have a profound effect on the measurement of GFR, even when using single-bolus techniques with plasma sampling, especially in patients with chronic kidney disease and edematous states.³⁵ In the rats that we used, the disease models included 5 of 6 nephrectomy and high-salt diets, which may have affected the volume of distribution and therefore the tGFR.¹⁹ Finally, bolus administration of

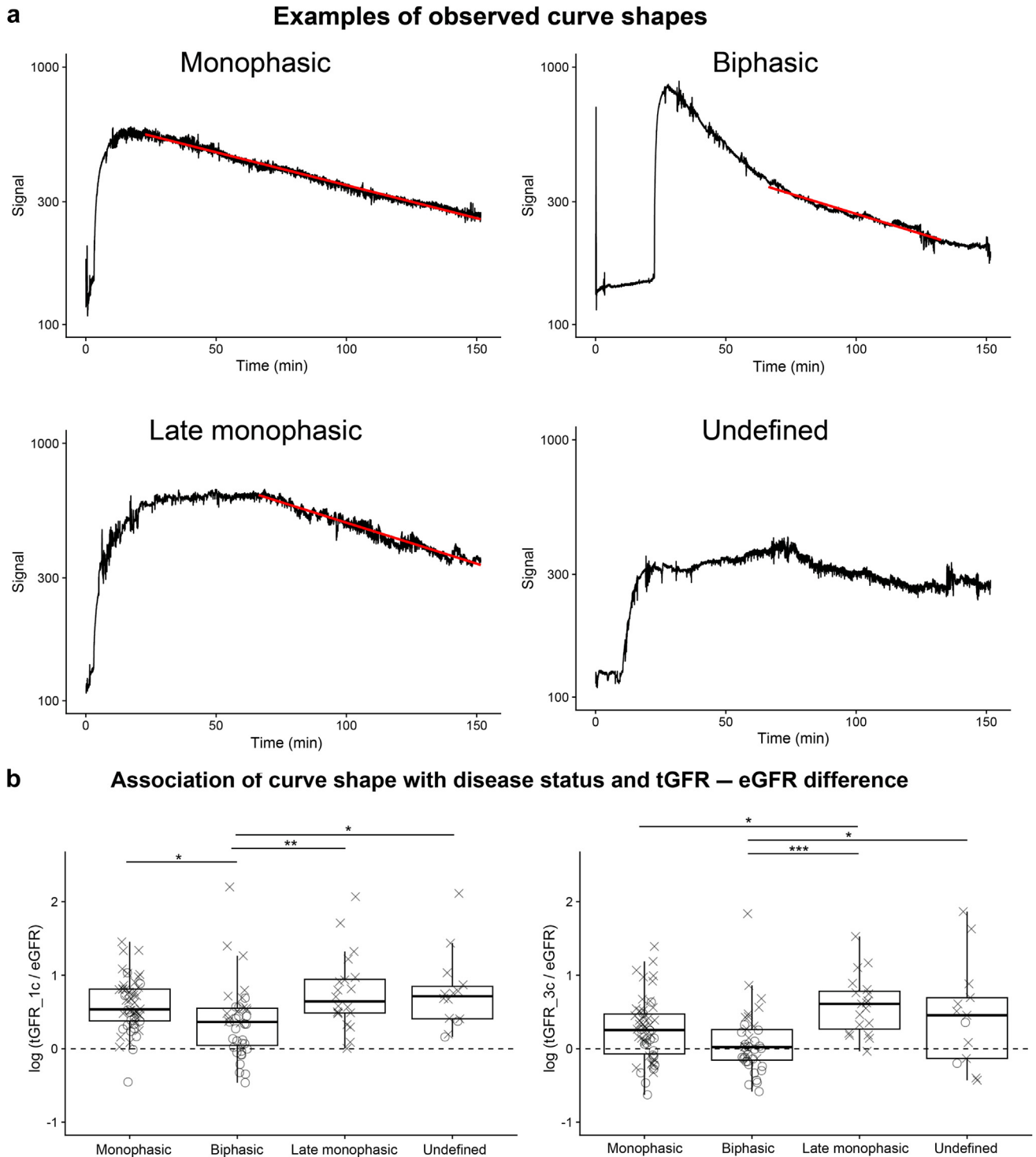


Figure 3 | (a) Examples of typical shapes of intensity curves with time in minutes on the x-axis, and signal on a log scale on the y-axis. The upper left panel shows monophasic elimination; the upper right panel shows biphasic elimination; the lower left panel shows late-monophasic elimination; and the lower right panel shows an undefined shape. The red line represents an ordinary least-squares regression line in the log-linear phase of the curve identified by eyeballing. **(b)** Association between curve shape with disease status and the difference between transcutaneous glomerular filtration rate (tGFR) – estimated glomerular filtration rate (eGFR). Boxplots comparing the log difference between tGFR, 1-compartment (tGFR_1c) – eGFR (left panel) and tGFR, 3-compartment (tGFR_3c) – eGFR (right panel) per curve shape, with open circles and crosses identifying whether the rat was in the control (open circle) or diseased group (cross). The log difference is a symmetric measure of the relative difference between tGFR – eGFR calculated as $\log(tGFR/eGFR)$; a log difference of 0 (indicated by the dotted line) indicates that eGFR and tGFR are equivalent. Differences between groups were compared with 2-way analysis of variance with factors curve shape and control versus diseased; significance is indicated as * $P < 0.05$, ** $P < 0.01$, and *** $P < 0.001$.

an exogenous tracer can result inadvertently in some extra-vascular administration, resulting in inappropriately high GFR measurements. This result was sometimes observed in control rats, but of course, it also could have occurred in diseased rats and thereby have contributed to the observed overlap.

This study has some shortcomings. A point to note is that the measurements of sinistrin clearance (mGFR), transcutaneous FITC-S clearance (tGFR), and plasma creatinine/urea for the calculation of eGFR were performed under different circumstances, which may have influenced our results. The mGFR was measured under isoflurane anesthesia, whereas the tGFR was measured in fully conscious animals. Theoretically, isoflurane may have caused depression of GFR by generalized hypotension and/or renal vasoconstriction. However, the mean arterial blood pressure was within the range of GFR autoregulation (80–160 mm Hg). An effect of isoflurane on GFR has never been reported in rats. One study reported that rats with halothane anesthesia had a reduced GFR (20% reduction), compared to that in conscious rats.³⁶ However, in humans, halothane has a much more profound effect on GFR than does isoflurane,³⁷ which suggests that the effect of isoflurane on GFR in rats most likely is minimal. If a decrease in GFR were to have occurred during anesthesia, this would have resulted in an increase in serum creatinine during the measurement of urinary sinistrin clearance, which we did not observe. Furthermore, the time between tGFR measurement and eGFR calculation may have influenced the results, if GFR substantially decreased in-between measurements (median 6 days). However, we included only chronic kidney disease models, in which such a dramatic decrease is not expected. In addition, we did not directly compare tGFR to the gold-standard mGFR, but rather to eGFR, which itself is an estimate. However, the clear bias and imprecision we observed are far greater than the bias and imprecision we saw in the validation study of the eGFR, and therefore, they are more likely caused by true disagreement between tGFR and mGFR than by inaccuracy of the eGFR equation. Furthermore, due to the retrospective nature of this study, we could not assess repeated measurements of tGFR and eGFR over time, which might have provided information on the variability of tGFR and eGFR measurements during disease progression. Additionally, we observed the discrepancy between tGFR and eGFR only during basal levels of kidney function. Future studies may address whether this discrepancy persists during physiological challenges, such as reflex activation of the baroreceptors or the somatosensory system.³⁸ Finally, we evaluated the tGFR in only male Sprague-Dawley rats in which chronic kidney disease was induced surgically; whether the divergence between eGFR and tGFR also is apparent in female rats or other strains and/or models is not clear.

The disagreement between tGFR and eGFR does not exclude the technique of transcutaneous kidney function measurements, and the repeated measurements of kidney function that this technique enables remain promising. Using different fluorophores, potentially in the near-infrared

spectrum (650–900 nm), might solve some of the technical challenges encountered with FITC-S.¹⁶ Further resolution of possible inaccuracy can be provided by directly comparing tGFR to the urinary clearance of other exogenous markers, such as iohexol or (FITC-)sinistrin, as currently, the tGFR has been validated against only transcutaneous plasma clearance with continuous infusion, in small groups of healthy rats¹⁷ and mice.³⁹ To compare tGFR with urinary FITC-S clearance in a large and diverse group of healthy and diseased rats, one could combine a single tGFR measurement with a continuous infusion and calculation of urinary FITC-S clearance in experiments in rats that use tGFR. Ideally, both the single tGFR measurement and the urinary FITC-S clearance should be performed under the same anesthetic regimen. The results of these papers also have implications for the use of tGFR in humans, as the fluorescent tracer MB-102 currently is being evaluated in a clinical trial in patients. Important considerations are the evaluation of the volume of distribution in different chronic kidney disease stages, and appropriate validation against a measure of mGFR, preferably against reliable measures of GFR, such as urinary clearance of an exogenous solute or plasma clearance with frequent sampling in the distribution phase.

In conclusion, this study shows that severe disagreement is present between GFR measured by transcutaneous FITC-S and eGFR. This inconsistency stresses the need for more-rigorous validation of the tGFR and, possibly, adjustments to the underlying technique.

DISCLOSURE

All the authors declared no competing interests.

DATA STATEMENT

The data that support the findings of this study are openly available at <https://doi.org/10.34894/8QYQZP>, DataverseNL, V1.

ACKNOWLEDGMENTS

The authors thank Diego O. Pastene Maldonado and the Core Facility of Preclinical Models, Mannheim, Germany, for help with fitting of the 3-compartment model. This study was supported by a grant to MCV and JAJ from the Netherlands CardioVascular Research Initiative—an initiative with the support of the Dutch Heart Foundation [CVON2014-11 (RECONNECT)]; a grant from ZonMw within the LSH 2Treat program and the Dutch Kidney Foundation [436001003 (InSiTeVx)] to MCV; and the Alexandre Suerman Stipend to TTP from the UMC Utrecht.

SUPPLEMENTARY MATERIAL

[Supplementary File \(PDF\)](#)

Supplementary Table S1. Included studies.

Supplementary Figure S1. Scatterplot depicting the stability of serum creatinine during anesthesia for the measurement of inulin clearance in the measured glomerular filtration rate (mGFR) cohort. The x-axis depicts serum creatinine ($\mu\text{mol/l}$) approximately 10–20 minutes after induction of anesthesia; the y-axis depicts serum creatinine at the end of the measurement period, approximately 1.5–2 hours after induction of anesthesia.

REFERENCES

- Nangaku M, Kitching AR, Boor P, et al. International Society of Nephrology first consensus guidance for preclinical animal studies in translational nephrology. *Kidney Int.* 2023;104:36–45.
- Levey AS, Coresh J, Tighiouart H, et al. Measured and estimated glomerular filtration rate: current status and future directions. *Nat Rev Nephrol.* 2020;16:51–64.
- Soveri I, Berg UB, Björk J, et al. Measuring GFR: a systematic review. *Am J Kidney Dis.* 2014;64:411–424.
- Dautzenberg M, Kahnert A, Stasch JP, Just A. Role of soluble guanylate cyclase in renal hemodynamics and autoregulation in the rat. *Am J Physiol Renal Physiol.* 2014;307:F1003–F1012.
- Schock-Kusch D, Sadick M, Henninger N, et al. Transcutaneous measurement of glomerular filtration rate using FITC-sinistrin in rats. *Nephrol Dial Transplant.* 2009;24:2997–3001.
- Besseling PJ, Pieters TT, Nguyen ITN, et al. A plasma creatinine- and urea-based equation to estimate glomerular filtration rate in rats. *Am J Physiol Renal Physiol.* 2021;320:518–524.
- Zhao C, Tang J, Li X, et al. Beneficial effects of procyanidin B2 on adriamycin-induced nephrotic syndrome mice: the multi-action mechanism for ameliorating glomerular permselectivity injury. *Food Funct.* 2022;13:8436–8464.
- Prado Y, Pérez L, Eltit F, et al. Procoagulant phenotype induced by oxidized high-density lipoprotein associates with acute kidney injury and death. *Thromb Res.* 2023;223:7–23.
- Jeddi S, Gheibi S, Kashfi K, Ghasemi A. Sodium hydrosulfide has no additive effects on nitrite-inhibited renal gluconeogenesis in type 2 diabetic rats. *Life Sci.* 2021;283:119870.
- Ahmed SA, Aziz WM, Shaker SE, et al. Urinary transferrin and proinflammatory markers predict the earliest diabetic nephropathy onset. *Biomarkers.* 2022;27:178–187.
- Sanad AM, Qadri F, Popova E, et al. Transgenic angiotensin-converting enzyme 2 overexpression in the rat vasculature protects kidneys from ageing-induced injury. *Kidney Int.* 2023;104:293–304.
- Han Z, Rao JS, Gangwar L, et al. Vitrification and nanowarming enable long-term organ cryopreservation and life-sustaining kidney transplantation in a rat model. *Nat Commun.* 2023;14:3407.
- Grashei M, Wodtke P, Skinner JG, et al. Simultaneous magnetic resonance imaging of pH, perfusion and renal filtration using hyperpolarized ¹³C-labelled Z-OMPD. *Nat Commun.* 2023;14:5060.
- Pill J, Issaeva O, Woderer S, et al. Pharmacological profile and toxicity of fluorescein-labelled sinistrin, a novel marker for GFR measurements. *Naunyn Schmiedeberg's Arch Pharmacol.* 2006;373:204–211.
- Schock-Kusch D, Xie Q, Shulhevich Y, et al. Transcutaneous assessment of renal function in conscious rats with a device for measuring FITC-sinistrin disappearance curves. *Kidney Int.* 2011;79:1254–1258.
- Huang J, Weinfurter S, Daniele C, et al. Zwitterionic near infrared fluorescent agents for noninvasive real-time transcutaneous assessment of kidney function. *Chem Sci.* 2017;8:2652–2660.
- Friedemann J, Heinrich R, Shulhevich Y, et al. Improved kinetic model for the transcutaneous measurement of glomerular filtration rate in experimental animals. *Kidney Int.* 2016;90:1377–1385.
- Huang J, Weinfurter S, Pinto PC, et al. Fluorescently labeled cyclodextrin derivatives as exogenous markers for real-time transcutaneous measurement of renal function. *Bioconjug Chem.* 2016;27:2513–2526.
- Bové DM, Uijl E, Severs D, et al. Dietary salt modifies the blood pressure response to renin-angiotensin inhibition in experimental chronic kidney disease. *Am J Physiol Renal Physiol.* 2021;320:F654–F668.
- Bové DM, Ren L, Uijl E, et al. Renoprotective effects of small interfering RNA targeting liver angiotensinogen in experimental chronic kidney disease. *Hypertension.* 2021;77:1600–1612.
- van Koppen A, Joles JA, van Balkom BWM, et al. Human embryonic mesenchymal stem cell-derived conditioned medium rescues kidney function in rats with established chronic kidney disease. *PLoS One.* 2012;7:1–12.
- van Koppen A, Joles JA, Bongartz LG, et al. Healthy bone marrow cells reduce progression of kidney failure better than CKD bone marrow cells in rats with established chronic kidney disease. *Cell Transplant.* 2012;21:2299–2312.
- van Koppen A, Verhaar MC, Bongartz LG, Joles JA. 5/6th nephrectomy in combination with high salt diet and nitric oxide synthase inhibition to induce chronic kidney disease in the Lewis rat. *J Vis Exp.* 2013;3:e50398.
- Papazova DA, Van Koppen A, Koeners MP, et al. Maintenance of hypertensive hemodynamics does not depend on ROS in established experimental chronic kidney disease. *PLoS One.* 2014;9:1–10.
- Van Koppen A, Papazova DA, Oosterhuis NR, et al. Ex vivo exposure of bone marrow from chronic kidney disease donor rats to pravastatin limits renal damage in recipient rats with chronic kidney disease. *Stem Cell Res Ther.* 2015;6:1–13.
- Koeners MP, Wesseling S, Sánchez M, et al. Perinatal inhibition of NF-KappaB has long-term antihypertensive and renoprotective effects in fawn-hooded hypertensive rats. *Am J Hypertens.* 2016;29:123–131.
- Emans TW, Patinha D, Joles JA, et al. Angiotensin II-induced hypertension in rats is only transiently accompanied by lower renal oxygenation. *Sci Rep.* 2018;8:1–9.
- Papazova DA, Krebber MM, Oosterhuis NR, et al. Dissecting recipient from donor contribution in experimental kidney transplantation: focus on endothelial proliferation and inflammation. *Dis Model Mech.* 2018;11:1–13.
- Nguyen ITN, Klooster A, Minnion M, et al. Sodium thiosulfate improves renal function and oxygenation in L-NNA-induced hypertension in rats. *Kidney Int.* 2020;98:366–377.
- Heyrovsky A. A new method for the determination of inulin in plasma and urine. *Clin Chim Acta.* 1956;1:470–474.
- Zöllner FG, Schock-Kusch D, Bäcker S, et al. Simultaneous measurement of kidney function by dynamic contrast enhanced MRI and FITC-sinistrin clearance in rats at 3 tesla: initial results. *PLoS One.* 2013;8:e79992.
- Mendelson Y, Ochs BD. Noninvasive pulse oximetry utilizing skin reflectance photoplethysmography. *IEEE Trans Biomed Eng.* 1988;35:798–805.
- Bashkatov AN, Genina EA, Kochubey VI, Tuchin VV. Optical properties of human skin, subcutaneous and mucous tissues in the wavelength range from 400 to 2000 nm. *J Phys D Appl Phys.* 2005;38:2543–2555.
- Peters AM. The kinetic basis of glomerular filtration rate measurement and new concepts of indexation to body size. *Eur J Nucl Med Mol Imaging.* 2004;31:137–149.
- White CA, Akbari A, Allen C, et al. Simultaneous glomerular filtration rate determination using inulin, iohexol, and ^{99m}Tc-DTPA demonstrates the need for customized measurement protocols. *Kidney Int.* 2021;99:957–966.
- Holstein-Rathlou NH, Christensen P, Leyssac PP. Effects of halothan+nitrous oxide inhalation anesthesia and Inactin on overall renal and tubular function in Sprague-Dawley and Wistar rats. *Acta Physiol Scand.* 1982;114:193–201.
- Colson P, Capdevilla X, Barlet H, et al. Effects of halothane and isoflurane on transient renal dysfunction associated with infrarenal aortic cross-clamping. *J Cardiothorac Vasc Anesth.* 1992;6:295–298.
- Johns EJ, Kopp UC, DiBona GF. Neural control of renal function. *Compr Physiol.* 2011;1:731–767.
- Mullins TP, Tan WS, Carter DA, Gallo LA. Validation of non-invasive transcutaneous measurement for glomerular filtration rate in lean and obese C57BL/6J mice. *Nephrology.* 2020;25:575–581.